Annals of Nuclear Medicine Vol. 17, No. 6, 481–488, 2003

Assessment of fatty acid metabolism in taxan-induced myocardial damage with iodine-123 BMIPP SPECT: Comparative study with myocardial perfusion, left ventricular function, and histopathological findings

Kimimasa SAITO,* Kan TAKEDA,** Kyoko IMANAKA-YOSHIDA,*** Hiroshi IMAI,***
Takao SEKINE**** and Yuko KAMIKURA****

*Department of Pulmonology, Yamada Red Cross Hospital
**Department of Radiology and ***Department of Pathology, Mie University
****Department of Internal Medicine, Matsusaka Central Hospital

We investigated myocardial fatty acid metabolism in taxan-induced myocardial damage in patients with advanced lung cancer. ***Patients and Methods:*** Twenty-five patients with non-small-cell lung cancer were treated with taxan combined with carboplatin intravenously for three cycles. Myocardial SPECT imaging using ^{99m}Tc-methoxyisobutyl isonitrile (MIBI) and ^{123}I-15-(*p*-iodophenyl)-3-(*R,S*)-methylpentadecanoic acid (BMIPP) was performed successively before and after chemotherapy. Regional uptake scores of BMIPP and MIBI were visually assessed and total uptake scores and the number of abnormal segments were calculated. Left ventricular ejection fraction (LVEF) was obtained by first-pass radionuclide angiocardiography using MIBI. Postmortem pathological examination was performed in 5 patients. ***Results:*** Total BMIPP uptake scores after chemotherapy were significantly lower than those before chemotherapy (23.4 ± 3.4 vs. 26.6 ± 0.8; $p < 0.001$). Mean LVEF showed a significant decrease after chemotherapy. Of the 25 patients, 4 exhibited a decrease in LVEF of more than 10%, 1 had a decrease in LVEF to below 50%, and 1 developed congestive heart failure. These 6 patients had significant decreases in total BMIPP uptake scores and increases in the number of abnormal segments as compared with the other 19 patients. Histopathological examination of myocardial tissue showed interstitial edema and disarrayed myocardial cells. ***Conclusion:*** Taxan impairs myocardial fatty acid metabolism. ^{123}I-BMIPP myocardial SPECT is useful for evaluating the cardiotoxicity induced by taxan.

Key words: ^{123}I-BMIPP, cardiotoxicity, paclitaxel, docetaxel, lung cancer

INTRODUCTION

PACLITAXEL (Taxol; Bristol-Myers Squibb Company, Princeton, NJ) and docetaxel (Taxotere; Aventis Pharmaceuticals, Inc., Parsippany, NJ) are members of the taxanes of pharmacologic agents that act by enhancing tubulin polymerization and inhibiting microtubule depolymerization. They have emerged as important agents in the treatment of lung, breast, and ovarian cancers. Taxan, however, has also been reported to cause severe cardiac toxic events such as arrhythmias, ischemia, and heart failure. It has been reported that 29% of paclitaxel-treated cancer patients develop cardiac abnormalities, leading to death in some cases.[1] Recently, as an important adverse effect, cardiac dysfunction has been observed with the use of paclitaxel plus a monoclonal antibody against HER2 (human epidermal growth factor receptor) for metastatic breast cancer.[2] Clinically, we encountered a patient who had been treated with six cycles of combined chemotherapy with paclitaxel and carboplatin for metastatic lung cancer originating from an ovarian tumor. She died of congestive heart failure. Histopathological examination of the autopsied heart showed severe interstitial edema and diffuse atrophy of myocardial cells. We

Received December 5, 2002, revision accepted June 16, 2003.
For reprint contact: Kimimasa Saito, M.D., Department of Pulmonology, Yamada Red Cross Hospital, 810 Takabuku, Misono, Watarai-gun, Mie 516–0805, JAPAN.
E-mail: k1saito@carrot.ocn.ne.jp

previously reported that ^{123}I-15-(*p*-iodophenyl)-3-(*R,S*)-methylpentadecanoic acid (BMIPP) myocardial dynamic single photon emission computed tomographic (SPECT) studies are useful for identifying patients at risk for doxorubicin cardiotoxicity in the early stages when cardiac function is still preserved.[3] In the present study, we therefore investigated fatty acid metabolism in taxan-induced myocardial damage using BMIPP SPECT imaging in comparison with myocardial perfusion evaluated by ^{99m}Tc-methoxyisobutyl isonitrile (MIBI) SPECT imaging, left ventricular function measurements, and histopathological findings.

PATIENTS AND METHODS

Subjects

This study was conducted in 25 patients with stage III or IV non-small-cell lung cancer. The mean age of the patients was 62.8 years, ranging from 40 to 78 years. The study group included 16 men and 9 women. None of the patients had previously received chemotherapy or had a history of diabetes mellitus or heart disease. No patients showed any abnormalities on the electrocardiogram (ECG) at rest or echocardiographic imaging. Written informed consent was obtained from all patients, and the study protocol was approved by the Institutional Review Board.

Chemotherapy protocols

In the docetaxel group, 16 patients were treated with 60 mg/m^2 of docetaxel combined with 300 mg/m^2 of carboplatin intravenously every 3 weeks for three cycles. In the paclitaxel group, 9 patients were treated with 180 mg/m^2 of paclitaxel combined with 300 mg/m^2 of carboplatin intravenously every 3 weeks for three cycles.

The premedication schedule for the paclitaxel group consisted of two doses of 20 mg each of dexamethasone by bolus intravenous injection at 12 and 6 hours before paclitaxel infusion. Patients were also premedicated with 50 mg of diphenhydramine orally plus 50 mg of ranitidine intravenously 30 minutes before paclitaxel infusion.

Instrumentation

Myocardial SPECT imaging was performed using a three-headed SPECT system (GCA-9300A; Toshiba Medical Systems, Tokyo, Japan) equipped with a high-resolution parallel-hole collimator. First-pass radionuclide angiocardiography was carried out using a dual-head SPECT system (GCA-7200A, Toshiba).

Study protocol

First-pass radionuclide angiocardiography and myocardial SPECT imaging with ^{99m}Tc-MIBI were performed successively 7 days before the initiation of chemotherapy. At least 2 days later, myocardial SPECT imaging with ^{123}I-BMIPP was carried out (2 to 4 days before the initiation of chemotherapy). The same protocol was repeated during the period from 10 to 17 days after the termination of chemotherapy.

Data acquisition

First-pass radionuclide angiocardiography

After the bolus injection of ^{99m}Tc-MIBI at 740 MBq, ECG-gated first-pass radionuclide angiocardiography was performed using a large-field gamma camera (GCA-7200A, Toshiba) with the patient in the supine position. Serial anterior chest images in the right anterior oblique view were obtained at a rate of 40 frames per second over 25 seconds. The matrix size was 64 × 64. The data were processed using an on-line computer (5500, Toshiba). The time-activity curves of the left ventricle were obtained and the LVEF values were calculated.

Myocardial SPECT imaging with ^{99m}Tc-MIBI

Thirty minutes after first-pass radionuclide angiocardiography, myocardial SPECT imaging with MIBI was performed. A total of 90 projection images were acquired over 360° in 4° increments with a 128 × 128 matrix. The total scan time was 12 minutes. Projection data were collected from a main window (140 keV ± 24%) and two 3% scatter rejection windows.

Myocardial SPECT imaging with ^{123}I-BMIPP

After breakfast on the day of the examination, all subjects

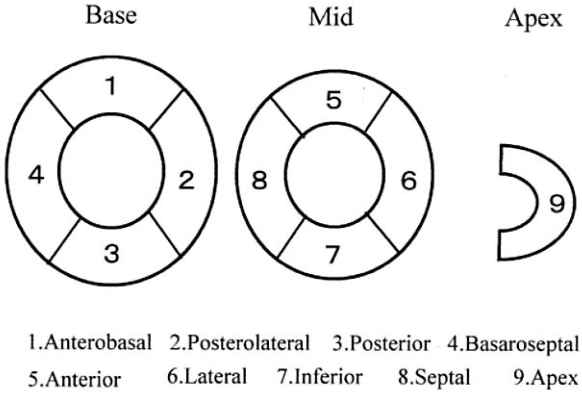

Fig. 1 Schematic representation of 9 segments of LV short-axial and vertical slices: 4 segments of a basal slice (anterobasal, posterolateral, posterior, and basaroseptal), 4 segments of a midventricular slice (anterior, lateral, inferior, and septal), and the apex.

Table 1 The changes of myocardial MIBI and BMIPP SPECT findings

	before–after	^{99m}Tc-MIBI (n = 25)	^{123}I-BMIPP (n = 25)
Unchanged	normal–normal	23 pts	9 pts
	abnormal–abnormal	1 pts	2 pts
Changed	worsening	1 pts	14 pts

were instructed to fast until completion of the study. Two hours after breakfast, 111 MBq of BMIPP was injected via an antecubital vein. Myocardial SPECT imaging was performed 30 minutes later. A total of 90 projection images were acquired over 360° in 4° increments with a 64 × 64 matrix. The data acquisition time was 20 seconds for each view. Projection data were collected from a main window (160 keV ± 12%) and two 3% scatter rejection windows.

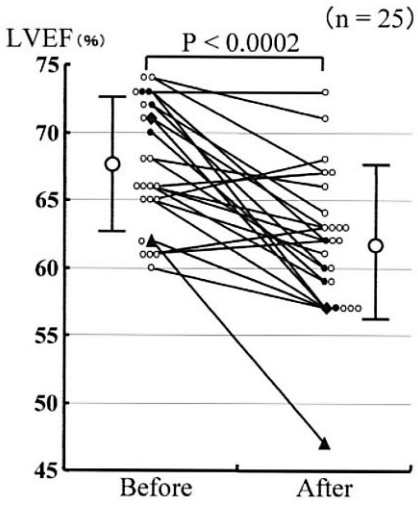

Fig. 2 Changes in LVEF before and after chemotherapy in 25 patients.

Image reconstruction

Transaxial tomographic images of the left ventricular myocardium were reconstructed using Butterworth and ramp filters for SPECT imaging with both ^{99m}Tc-MIBI and ^{123}I-BMIPP. The matrix size was 128 × 128. Scatter correction was performed using the triple-energy window method,[4] but no attenuation correction was done. Short-axial, vertical long, and horizontal images of the left ventricular myocardium were reconstructed with a slice thickness of 12.8 mm.

Data analysis

Visual assessment of SPECT images with MIBI and BMIPP

The LV myocardium was divided into 9 segments as shown in Figure 1. ^{99m}Tc-MIBI and ^{123}I-BMIPP SPECT images were visually assessed and the regional uptake

Table 2 Outcome of all 25 patients

Patient No.	Sex/Age	Drug	Total dose (mg/m^2)	LVEF of FPRA		^{123}I-BMIPP				Cardiotoxicity grade
				Before (%)	After (%)	Total score		Abnormal seg.		
						Before	After	Before	After	
1	M/72	P	540	73	62	26	20	1	5	I
2	M/53	P	540	72	60	27	20	0	5	I
3	F/61	D	180	73	57	26	20	1	4	I
4	M/79	D	180	70	59	27	17	0	6	I
5	M/40	D	180	62	47	27	22	0	3	II
6	F/50	D	180	71	57	27	20	0	5	III
mean	63.8 ± 15.4			70.2	57.0	26.7	19.8	0.3	4.7	
7	M/61	P	540	74	67	27	27	0	0	0
8	F/72	P	540	66	67	27	27	0	0	0
9	M/75	P	540	61	63	27	27	0	0	0
10	M/68	P	540	68	60	27	22	0	3	0
11	F/51	P	540	71	63	27	18	0	5	0
12	M/54	P	540	66	63	27	27	0	0	0
13	F/67	P	540	65	61	26	26	1	1	0
14	M/69	D	180	65	68	27	27	0	0	0
15	F/41	D	180	66	59	26	25	1	2	0
16	M/61	D	180	65	57	27	19	0	6	0
17	M/62	D	180	62	57	26	22	1	3	0
18	M/60	D	180	60	57	24	21	1	2	0
19	M/70	D	180	61	62	27	27	0	0	0
20	M/71	D	180	61	63	27	23	0	3	0
21	M/59	D	180	72	64	27	24	0	2	0
22	F/48	D	180	73	73	27	27	0	0	0
23	F/63	D	180	68	66	27	27	0	0	0
24	F/71	D	180	66	62	25	25	1	1	0
25	M/67	D	180	74	71	27	27	0	0	0
mean	62.6 ± 9.0			66.5	63.3	26.6	24.6	0.3	1.5	

Abbreviation: Drug D, docetaxel; P, paclitaxel; LVEF, left ventricular ejection fraction; FPRA, first pass radioangiography; seg., segments

score for each segment was determined using a 4-point scale (0 = absent, 1 = moderately reduced, 2 = mildly reduced, 3 = normal) based on the consensus of three experienced observers. Disagreement among the observers was resolved by consensus. Total MIBI and BMIPP uptake scores were calculated by summing the regional uptake scores of the 9 segments. The number of abnormal segments with a regional uptake score of less than 3 was determined for both MIBI and BMIPP SPECT images.

Criteria for toxicity

The National Cancer Institute (NCI) common toxicity criteria (Version 2.0, Jan. 30, 1998) were employed to evaluate the cardiac toxicity of taxan in this study as follows.

Grade 0: Normal.

Grade 1: Asymptomatic decline in resting ejection fraction of ≥10% but <20% of the baseline value.

Grade 2: Asymptomatic, but the resting ejection fraction is below the lower limit (50%) of normal for the laboratory, or a decline in resting ejection fraction of ≥20%.

Grade 3: CHF responsive to treatment.

Grade 4: Severe CHF refractory to treatment or requiring intubation.

Histopathological analysis

Seven of the 25 patients died during the study. Five autopsies were performed. Myocardial samples were obtained from the anterior left ventricular wall. The tissues were fixed with 10% formalin and embedded in paraffin. Sections were cut at 3 μm and stained with hematoxylin-eosin.

Statistical analysis

All data are presented as a mean ± standard deviation (s.d.). Wilcoxon's signed-ranks test was applied to test the differences in LVEF, total scores, and the number of abnormal segments in ^{123}I-BMIPP before and after chemotherapy. Mann-Whitney's U test was used to compare the differences in total scores or the number of abnormal segments of BMIPP SPECT images between the patients assigned to the grade = 0 group and the grade ≥1 group. Differences with $p < 0.05$ were considered statistically significant.

RESULTS

Changes in MIBI and BMIPP SPECT findings before and after chemotherapy

The changes of myocardial MIBI and BMIPP SPECT findings before and after chemotherapy are summarized in Table 1. Most patients (23/25, 92%) showed normal perfusion on MIBI SPECT images both before and after chemotherapy. On BMIPP SPECT images, in contrast, 9 patients (36%) showed normal uptake both before and after chemotherapy, but 14 patients (56%) showed worsening of BMIPP SPECT images after chemotherapy.

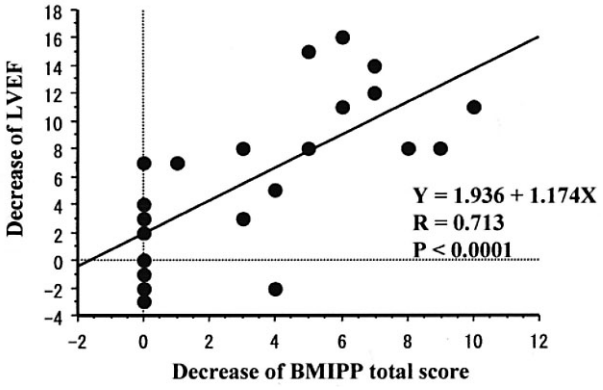

Fig. 3 Relationship between the fractional change in the LVEF and decrease BMIPP uptake scores after chemotherapy.

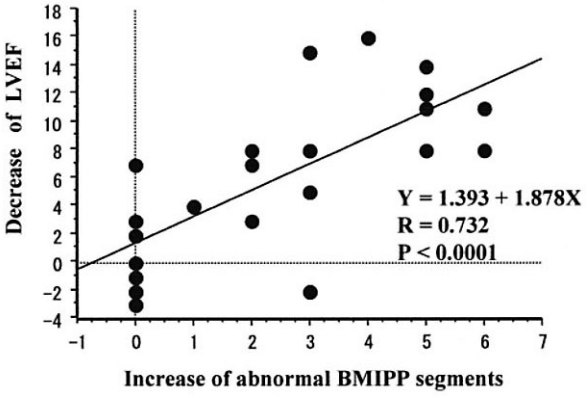

Fig. 4 Relationship between the fractional change in the LVEF and increase BMIPP abnormal segments after chemotherapy.

The numbers of segments which showed deterioration on BMIPP SPECT images after chemotherapy, from segmemt 1 to 9 were 7, 5, 10, 7, 3, 3, 11, 5, 5 respectively. The disordered areas were diffusely distributed over all segments, with a tendency seen in inferior segments.

Comparison of total MIBI and BMIPP scores before and after chemotherapy

Although there were no significant changes in total MIBI uptake scores before and after chemotherapy (26.9 ± 0.2 vs. 26.8 ± 0.4, NS), total BMIPP uptake scores showed a significant decrease after chemotherapy compared with before chemotherapy (23.4 ± 3.4 vs. 26.6 ± 0.8, $p < 0.001$). The number of abnormal segments in BMIPP showed a significant increase after chemotherapy compared with before chemotherapy (2.24 ± 2.2 vs. 0.28 ± 0.5, $p < 0.0009$).

Table 3 Pathological findings of the 5 patients

	Patients no.				
	13	16	19	21	6
Age	67	61	70	59	78
Total dose of taxan (mg)	360	240	180	180	180
History x of CHF	–	–	–	–	○
Atrophy of heart muscle	++	++	++	+	+
Interstitial edema	+	+	+	+	+
Disarray orientation of myofibers	+	+	+	–	–
Fibrosis	–	–	–	–	–

Abbreviation: CHF, congestive heart failure
++, marked; +, mild

Comparison of LVEF values before and after chemotherapy

Fractional changes in LVEF evaluated by first-pass radionuclide angiocardiography before and after chemotherapy are presented in Figure 2. The mean LVEF was 66.9% ± 4.8% before chemotherapy and 60.6% ± 4.8% after chemotherapy. A significant decrease in LVEF was observed after chemotherapy ($p < 0.0002$). Four patients exhibited a decrease in LVEF of more than 10% (grade 1 toxicity) after chemotherapy (solid circles) (●), one patient (solid triangles) (▲) had a decrease in LVEF to below 50% (grade 2 toxicity), and one patient (solid diamonds) (◆) developed congestive heart failure 26 days after the final administration (grade 3 toxicity). Based on the NCI common toxicity criteria, these 6 patients were classified as showing evidence of cardiotoxicity.

Clinical findings and outcome in the 25 patients

The type of taxan, administered dose, LVEF, BMIPP findings before and after chemotherapy, and cardiotoxicity grades are summarized in Table 2. The patients received 540 mg/m^2 of paclitaxel or 180 mg/m^2 of docetaxel. It is considered that 2.5 mg of paclitaxel is equivalent to 1 mg of docetaxel.[5] We divided the patients into two groups: group 1 (6 patients) in which grade 1 cardiotoxicity or greater was observed, and group 2 (19 patients) in which the cardiotoxicity criteria were not met (Grade 0). These two groups were compared.

Total BMIPP uptake scores after chemotherapy were significantly lower in group 1 than in group 2 (19.8 ± 1.6 vs. 24.6 ± 3.0, $p < 0.004$). The number of abnormal segments in BMIPP SPECT images after chemotherapy was significantly higher in group 1 than in group 2 (4.7 ± 1.0 vs. 1.5 ± 1.9, $p < 0.001$).

The decrease of LVEF was plotted against the decrease in the total BMIPP score, with a significant linear correlation observed ($r = 0.713$, $p < 0.0001$; Fig. 3).

The decrease of LVEF was plotted against the increase in the number of abnormal BMIPP segments, and a significant linear correlation was observed ($r = 0.732$, $p < 0.0001$; Fig. 4).

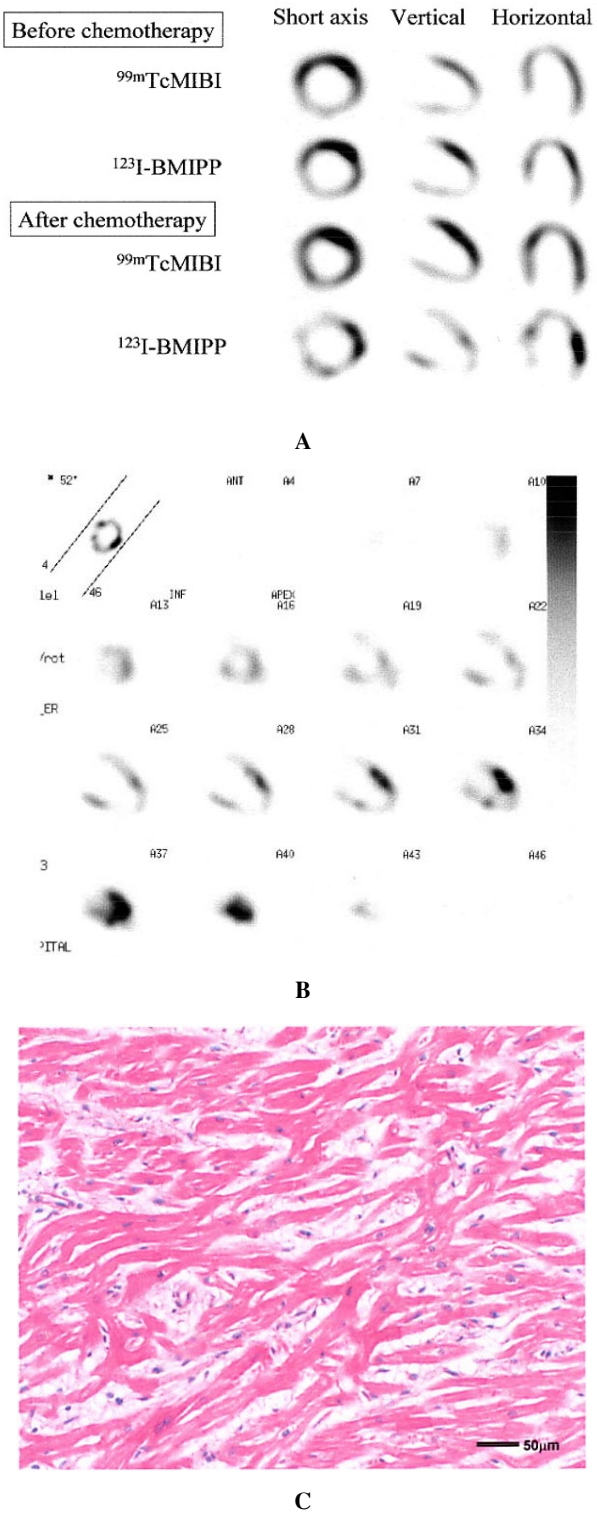

Fig. 5 (A) MIBI and BMIPP myocardial SPECT images before and after chemotherapy. (B) All vertical slices of BMIPP SPECT images after chemotherapy show multiple patchy areas of decreased uptake. (C) In a histological section of the myocardium. (Scale bar: 50 μm)

Histopathological findings

Histopathological findings for the myocardium in the 5 patients who underwent postmortem pathological examination are summarized in Table 3. These patients ranged in age from 59 to 78 years. One patient (Patient No. 13) was treated with a combination of paclitaxel and carboplatin, and the other 4 patients were treated with a combination of docetaxel and carboplatin. Some cycles of chemotherapy were repeated in 2 of these patients. One patient (Patient No. 6) developed congestive heart failure. Four patients died of cancer and 1 patient (Patient No. 16) of hemoptysis. The myocardial tissue from all 5 patients showed atrophy of myocardial cells and interstitial edema. Disarrayed myocardial cells were observed in 3 patients. These pathological findings were diffusely distributed throughout the myocardium. The extent of these morphological changes tended to correlate with the total administered dose of taxan. No vacuolar degeneration, interstitial fibrosis, or infiltration of inflammatory cells were detected.

Case presentation

A 61-year-old man with lung cancer (Patient No. 16 in Tables 2 and 3) is shown as a representative case in Figure 5. He was treated with 60 mg/m^2 of docetaxel combined with 300 mg/m^2 of carboplatin intravenously every 3 weeks for three cycles. The total dose of docetaxel administered was 180 mg/m^2 at the time of examination. The LVEF was decreased to 57% after chemotherapy from 65% before chemotherapy. Figure 5 (A) shows MIBI and BMIPP myocardial SPECT images before and after chemotherapy. Myocardial perfusion and BMIPP uptake were normal before chemotherapy. Although myocardial perfusion appears normal even after chemotherapy, the BMIPP images show a patchy decrease in uptake in the anterobasal and inferior segments. Figure 5 (B) shows all vertical slices of BMIPP SPECT images after chemotherapy. These images show multiple areas of patchy decrease in BMIPP uptake distributed throughout the left ventricle. The patient died on the 90th day after the final administration of docetaxel. The total amount of docetaxel administered was 240 mg/m^2. Autopsy was performed and histopathological examination confirmed atrophy of the myocardial cells, disarrayed myocardial cells, and interstitial edema (Fig. 5 (C)).

DISCUSSION

Myocardial damage induced by taxan

Although few published reports have described drug-induced myocardial contractile dysfunction caused by combination chemotherapy with taxan and carboplatin, many reports are available on the cardiotoxicity of the combination of taxan and doxorubicin. The incidence of myocardial damage has been reported to be about 2% to 30%,[6–11] and serious cases have frequently been observed. According to these studies, there was a higher incidence of a decrease in LVEF by 10% or more or the development of congestive heart failure after chemotherapy, compared with retrospectively derived historical data of doxorubicin cardiomyopathy. This synergism could result from a pharmacokinetic interaction between taxan and other drugs resulting in a decreased clearance of either doxorubicin or the doxorubicin metabolite doxorubicinol, as suggested by pharmacokinetic studies performed by Minotti et al.[12] and Berg et al.[13] On the other hand, several groups have reported data concerning single-agent chemotherapy with taxan. Chang et al. reported that 4 of 24 (17%) patients treated with paclitaxel at 250 mg/m^2 every 3 weeks developed grade 3 or greater cardiotoxicity.[14] Chan et al. reported that 7 of 86 patients (8%) treated with docetaxel at 100 mg/m^2 every 3 weeks showed a decrease in LVEF by more than 20%.[15,16] Kavanagh et al. reported that 5 of 55 patients (9%) treated with docetaxel at 100 mg/m^2 every 3 weeks experienced cardiac events.[17] In our series, 4 of 25 patients (16%) exhibited a decrease in LVEF by more than 10%, 1 patient (4%) had a decrease of LVEF below 50%, and 1 patient (4%) developed congestive heart failure after combination chemotherapy with taxan and carboplatin. Although the number of patients in our study was limited, the incidence rate of myocardial damage appears to be comparable to the results reported in previously published papers.

Myocardial MIBI and BMIPP SPECT images

The comparative study of myocardial MIBI and BMIPP SPECT findings described in this report demonstrated that combination therapy with taxan and carboplatin did not affect myocardial perfusion but could impair fatty acid metabolism. In 14 of 25 patients (56%), myocardial BMIPP SPECT images worsened after chemotherapy. In our previous study,[3] myocardial BMIPP SPECT imaging was performed in cancer patients treated with doxorubicin. It was concluded that chemotherapy with doxorubicin was not associated with any abnormality in myocardial BMIPP SPECT images and that dynamic SPECT study using ^{123}I-BMIPP was necessary to evaluate impaired myocardial fatty acid metabolism. Based on the results of these two studies, taxan combined with carboplatin appears to exert a more toxic effect on myocardial fatty acid metabolism than doxorubicin.

Furthermore, both total uptake scores and the number of abnormal segments in BMIPP became significantly worse in the Grade ≥ 1 group, based on the NCI common toxicity criteria, compared with the Grade = 0 group. The decrease of LVEF and aggravation of BMIPP SPECT images showed a significant linear correlation. These findings suggest that combination therapy with taxan and carboplatin causes an impairment in myocardial fatty acid metabolism as well as myocardial contractile dysfunction.

Pathological findings in taxan-induced myocardial damage

Several reports have documented the morphological changes in taxan-induced myocardial damage. Jekunen et al.[18] reported that electron microscopy revealed peculiar subsarcolemmal concentric lamellar bodies, although light microscopy showed no changes. Sheck et al.[19] also noted swelling of the sarcoplasmic reticulum, loss of myofibrils, an accumulation of lipofuscin, and laminated myelinoid figures by electron microscopy. At the light microscopic level, they also described focal vacuolar degeneration surrounded by a few hypertrophic myocytes with enlarged hyperchromatic nuclei. Both patients in their report had previously received anthracycline or anthraquinone anti-cancer drugs, which have been identified as cardiotoxic agents.

In the present study, atrophy of myocardial cells and interstitial edema were observed in all 5 patients who underwent postmortem pathological examination. Disarrayed myocardial cells were also observed in 3 patients. These changes were not localized to the endomyocardium but were diffusely distributed. The ubiquitous distribution of the lesions suggests that these changes may not be due to impaired blood flow, which is consistent with the finding on MIBI SPECT images that myocardial perfusion was not impaired. Furthermore, the severity of interstitial edema and disarrayed myocardial cells was greater in patients that received larger doses of taxan. These results suggest that there may be some dose-dependency in the cardiotoxicity induced by taxan.

Myocardial disorder caused by either doxorubicin or taxan becomes irreversible when fibrosis occurs. In the disorder process, doxorubicin causes a decrease of mitochondrial function in the myocardial cell.[20] On the other hand taxan causes hypergasia of the microtuble which should become fatty acid transport meridian. We thought that a difference in this process accounted for the distinction of BMIPP static image. Even if these biochemical mechanisms are responsible, myocardial cells could undergo apotosis finally. Therefore, vacuolation should be recognized in these histopathological findings. In a previous paper, vacuolation was reported as a myocardial disorder caused by doxorubicin. In addition, Sheck et al. presented it as a characteristic finding on light microscopy of myocardial disorder caused by taxan.[19]

In our study, tissue examination was limited to light microscopy, and therefore we think that the histopathological findings are insufficient to completely explain the mechanism of cardiotoxicity.

Mechanism speculated to be responsible for the cardiotoxicity induced by taxan

In a cancer cell, taxan promotes microtubule assembly and inhibits microtubule depolymerization, thereby causing an increase in nonfunctional microtubules. In the myocardium, taxan is known to induce impaired contractility. Lampidis et al. have described the alterations in microtubular assembly that were found to affect the contractile function of newborn rat cardiac cells in culture.[21] Tsutsui et al. reported that paclitaxel caused a decline of the velocity of sarcomere shortening in cardiocytes isolated from normal cats.[22] Zile et al. reported that paclitaxel caused a contractile defect in normal papillary muscles isolated from cats.[23] The mechanism of this contractile dysfunction has been explained by an increase in the density of the cellular microtubule network which may counterbalance the contractile force exerted by actin-myosin cross bridges.[24]

Furthermore, it is generally accepted that microtubules function as a railway conduit that transports cargo particles between the sites where lipid and protein particles are synthesized and the target organelles under construction.[25] In fact, in cardiomyocytes, the microtubular array serves as a tract for the transport of components of the sarcoplasmic reticulum.[26] If this normal microtubular transport system is impaired by the administration of taxan, the free fatty acids produced may not be stored in the lipid pool of the cytosol, and as a result, uptake by the mitochondria may be reduced. This could be reflected by a decrease in the uptake of ^{123}I-BMIPP. If this is the case, BMIPP SPECT images would permit the early detection of cardiotoxicity caused by taxan.

CONCLUSIONS

Taxan was found to impair myocardial fatty acid metabolism without affecting myocardial perfusion. ^{123}I-BMIPP myocardial SPECT is useful for evaluating the cardiotoxicity induced by taxan.

REFERENCES

1. Rowinsky EK, McGuire WP, Guarnieri T, Fisherman JS, Christian MC, Donehower RC. Cardiac disturbances during the administration of Taxol. *J Clin Oncol* 1991; 9: 1704–1712.
2. Slamon DJ, Leyland-Jones B, Shak S, Fuchs H, Paton V, Bajamonde A, et al. Use of chemotherapy plus a monoclonal antibody against HER2 for metastatic breast cancer that overexpresses HER2. *N Engl J Med* 2001; 344: 783–792.
3. Saito K, Takeda K, Okamoto S, Okamoto R, Makino K, Tameda Y, et al. Detection of doxorubicin cardiotoxicity by using iodine-123 BMIPP early dynamic SPECT: Quantitative evaluation of early abnormality of fatty acid metabolism with the Rutland method. *J Nucl Cardiol* 2000; 7: 553–561.
4. Ichihara T, Ogawa K, Motomura N, Kubo A, Hashimoto S. Compton scatter compensation using the triple-energy window method for single- and dual-isotope SPECT. *J Nucl Med* 1993; 34: 2216–2221.
5. Robert TD. Pharmacology of the taxanes. *Pharmacology* 1997; 5 (suppl): 96–104.
6. Sparano JA. Doxorubicin/taxane combinations: Cardiac

toxicity and pharmacokinetics. *Semin Oncol* 1999; 26 (suppl): 14–19.
7. Gianni L, Munzone E, Capri G, Fulfaro F, Tarenzi E, Villani F, et al. Paclitaxel by 3-hour infusion in combination with bolus doxorubicin in women with untreated metastatic breast cancer: High antitumor efficacy and cardiac effects in dose-finding and sequence-finding study. *J Clin Oncol* 1995; 13: 2688–2699.
8. Dombernowsky P, Gehl J, Boesgaard M, Paaske T, Jensen BV. Doxorubicin and Paclitaxel, a highly active combination in the treatment of metastatic breast cancer. *Semin Oncol* 1996; 23 (suppl): 23–27.
9. Conte PF, Baldini E, Gennari A, Michelotti A, Salvadori B, Tibaldi C, et al. Dose-finding study and pharmacokinetics of epirubicin and paclitaxel over 3 hours: A regimen with high activity and low cardiotoxicity in advanced breast cancer. *J Clin Oncol* 1997; 15: 2510–2517.
10. Sparano JA. Use of dexrazoxane and other strategies to prevent cardiomyopathy associated with doxorubicin-taxane combinations. *Semin Oncol* 1998; 25 (suppl): 66–71.
11. Nabholtz JM, Tonkin K, Smylie M, Mackey J, Janowska-Wieczorek A. Review of docetaxel and doxorubicin-based combinations in management of breast cancer: From metastatic to adjuvant setting. *Semin Oncol* 1999; 26 (suppl): 10–16.
12. Minotti G, Sponiero A, Licta S, Menna P, Calafiore AM, Teodori G, et al. Paclitaxel and docetaxel enhance the metabolism of doxorubicin to toxic species in human myocardium. *Clin Cancer Res* 2001; 7: 1511–1515.
13. Berg SL, Cowan KH, Balis FM, Fisherman JS, Denicoff AM, Hillig M, et al. Pharmacokinetics of Taxol and doxorubicin administered alone and in combination by continuous 72-hour infusion. *J Natl Cancer Inst* 1994; 86: 143–145.
14. Chang AY, Kim K, Glick J, Anderson T, Karp D, Johnson D. Phase II study of Taxol, merbarone, and piroxantrone in stage IV non-small-cell lung cancer: The Eastern Cooperative Oncology Group results. *J Natl Cancer Inst* 1993; 85: 388–394.
15. Chan S, Friedrichs K, Noel D, Pintér T, Belle SV, Vorobiof D, et al. Prospective randomized trial of docetaxel versus doxorubicin in patients with metastatic breast cancer. *J Clin Oncol* 1999; 17: 2341–2354.
16. Crown J. Phase III randomized trials of docetaxel in patients with metastatic breast cancer. *Semin Oncol* 1999; 26 (suppl): 33–38.
17. Kavanagh JJ, Kudelka AP, Leon CG, Tresukosol D, Hord M, Finnegan B, et al. Phase II study of docetaxel in patients with epithelial ovarian carcinoma refractory to platinum. *Clinical Cancer Research* 1996; 2: 837–842.
18. Jekunen A, Heikkila P, Malche A, Pyrhönen S. Paclitaxel-induced myocardial damage detected by electron microscopy. *Lancet* 1994; 343 (letter): 727–728.
19. Sheck TW, Luk IS, Ma L, Cheung KL. Paclitaxel-induced cardiotoxity. An ultrastructual study. *Arch Pathol Lab Med* 1996; 120: 89–91.
20. Erland JFD, Poul KJ. Destruction of phospholipids and respiratory-chain activity in pig-heart submitochondrial particles induced by an adriamycin-iron complex. *Eur J Biochem* 1983; 132: 551–556.
21. Lampidis TJ, Kolonias D, Savaraj N, Rubin RW. Cardiostimulatory and antiarrhythmic activity of tubulin-binding agents. *Proc Natl Acad Sci* 1992; 89: 1256–1260.
22. Tsutsui H, Ishihara K, Cooper G. Cytoskeletal role in the contractile dysfunction of hypertrophied myocardium. *Science* 1993; 260: 682–687.
23. Zile MR, Koide M, Sato H, Ishiguro Y, Conrad CH, Buckley JM, et al. Role of microtubules in the contractile dysfunction of hypertrophied myocardium. *J Am Coll Cardiol* 1999; 33: 250–260.
24. Danowski BA. Fibroblast contractility and actin organization are stimulated by microtubule inhibitors. *J Cell Sci* 1989; 93: 255–266.
25. Hirokawa H. Kinesin and dynein superfamily proteins and the mechanism of organelle transport. *Science* 1998; 279: 519–526.
26. Ioshii SO, Imanaka-Yoshida K, Yoshida T. Organization of calsequestrin-positive sarcoplasmic reticulum in rat cardiomyocytes in culture. *J Cell Physiol* 1994; 158: 87–96.